CSIRO PUBLISHING

Full Paper

www.publish.csiro.au/journals/ajc

Aust. J. Chem. **2010**, *63*, 687–692

Supramolecular Chemistry of Pyronines B and Y, β-Cyclodextrin and Linked β-Cyclodextrin Dimers

Huy T. Ngo,[A] *Philip Clements,*[A] *Christopher J. Easton,*[B] *Duc-Truc Pham,*[A] *and Stephen F. Lincoln*[A,C]

[A]School of Chemistry and Physics, University of Adelaide, Adelaide, SA 5005, Australia.
[B]Research School of Chemistry, Australian National University, Canberra, ACT 0200, Australia.
[C]Corresponding author. Email: stephen.lincoln@adelaide.edu.au

The complexation of cationic pyronine B (PB^+) and pyronine Y (PY^+) by β-cyclodextrin (βCD) and two linked βCD dimers, *N*,*N*′-bis((2^{A}S,3^{A}S)-3^A-deoxy-β-cyclodextrin-3^A-yl)succinamide, 33βCD_2suc, and *N*,*N*′-bis(6^A-deoxy-β-cyclodextrin-6^A-yl)succinamide, 66βCD_2suc, in aqueous solution has been studied by UV-vis, fluorescence, and ^{1}H NMR spectroscopy. The complexation constants for the 1:1 complexes: βCD.PB^+, 33βCD_2suc.PB^+, 66βCD_2suc.PB^+, and the analogous PY^+ complexes are reported as are the dimerization constants for PB^+ and PY^+. The modes of complexation, dimerization, and fluorescence quenching are discussed.

Manuscript received: 2 September 2009.
Manuscript accepted: 7 January 2010.

Introduction

Native and modified cyclodextrins act as robust hosts for a wide variety of guest species in water.[1–4] Consequently, they are at the centre of supramolecular chemistry, where secondary bonding between interacting host and guest species modifies the chemical and physical behaviour of both in proportion to the strength of interaction. Native cyclodextins and a range of their modified forms are biocompatible which, in combination with their supramolecular host characteristics, results in many thousands of tonnes being used in industry annually.[5–8]

Often in supramolecular systems, several competing equilibria exist, as exemplified by host-guest complexation and guest aggregation. In this study, we simultaneously quantify the complexation of the dimerizing cationic pyronines B and Y, PB^+ and PY^+, by β-cyclodextrin, βCD, and the modified cyclodextrins *N*,*N*′-bis((2^{A}S,3^{A}S)-3^A-deoxy-β-cyclodextrin-3^A-yl)succinamide, 33βCD_2suc, and *N*,*N*′-bis(6^A-deoxy-β-cyclodextrin-6^A-yl)succinamide, 66βCD_2suc, in which a succinamide linker joins two βCDs through either the C_3^A or C_6^A carbons of altropyranose and glucopyranose units, respectively (Fig. 1).[9] These systems are chosen because the structural differences among the host and guest species are expected to give insight into host-guest complexation of PB^+ and PY^+, their dimerization, and the factors affecting their fluorescence, which is the subject of debate.[10–16]

Results and Discussion

Equilibria

$$33\beta CD_2suc + PB^+ \underset{}{\overset{K_1}{\rightleftharpoons}} 33\beta CD_2.PB^+ \quad (1)$$

$$2PB^+ \underset{}{\overset{K_d}{\rightleftharpoons}} (PB^+)_2 \quad (2)$$

Equilibria (1) and (2), characterized by UV-vis, fluorescence, and ^{1}H NMR spectroscopy, dominate the 33βCD_2suc/PB^+ system and analogous equilibria apply to the other five systems. The derived equilibrium constants K_1 and K_d appear in Table 1. There is reasonable agreement between the K_1 derived through all three techniques.

UV-vis and Fluorescence Studies

The variations of the UV-vis and fluorescence spectra of PB^+ and PY^+ with increasing concentrations of βCD, 33βCD_2suc and 66βCD_2suc, are typified by the data for the 33βCD_2suc/PB^+ system shown in Figs 2 and 3, respectively. A red shift of the absorption and emission maxima of PB^+ occurs together with a decrease in both absorbance and fluorescence intensity as $[33\beta CD_2suc]_{total}$ increases. The isosbestic point at 556 nm (Fig. 2) is consistent with PB^+ existing predominantly in the free and 33βCD_2suc.PB^+ complexed states, in an equilibrium characterized by K_1 (Eqn 1). An algorithm for the formation of the 1:1 complex 33βCD_2suc.PB^+ best-fits the data at 0.5 nm intervals, in the range 500–590 nm, to yield $K_1 = 4200 \pm 200\ dm^3\ mol^{-1}$. The decrease in fluorescence of PB^+ with increasing $[33\beta CD_2suc]_{total}$ in Fig. 3 was similarly best-fitted over the range 540–650 nm, to give $K_1 = 4600 \pm 200\ dm^3\ mol^{-1}$. The K_1 for the other five systems (Table 1) were similarly derived.

The K_1 for the complexation of PB^+ and PY^+ by 33βCD_2suc and 66βCD_2suc are slightly more than twice the K_1 for complexation by βCD. This indicates that 33βCD_2suc and 66βCD_2suc have little more than a statistical advantage in forming host-guest complexes over βCD. However, PB^+ is complexed approximately five times more strongly than PY^+, consistent with the ethyl groups extending the hydrophobicity of PB^+ by a greater amount to interact more strongly with the hydrophobic annuli of βCD, 33βCD_2suc, and 66βCD_2suc, than do the methyl groups of PY^+. The differing stereochemistries of 33βCD_2suc and 66βCD_2suc have little effect on complexation, despite the

 10.1071/CH09467 0004-9425/10/040687

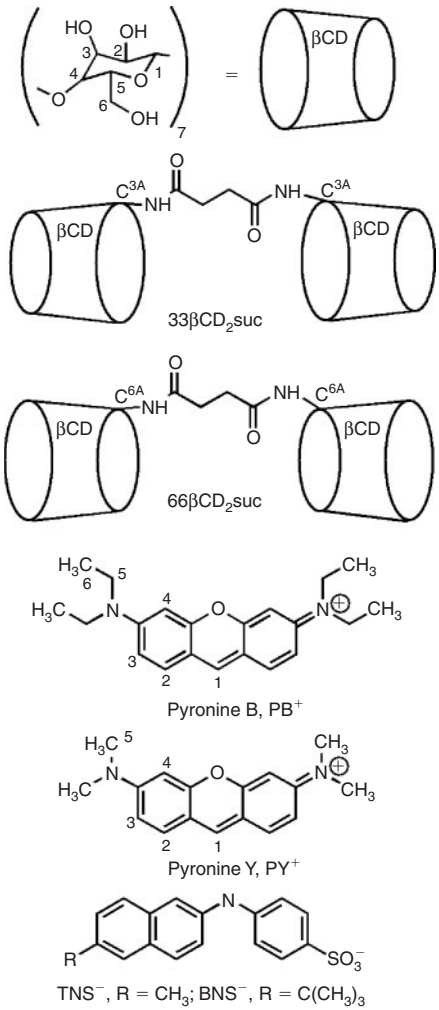

Fig. 1. Structures of βCD, 33βCD$_2$suc, 66βCD$_2$suc, PB$^+$, PY$^+$, BNS$^-$, and TNS$^-$.

inversions at the C_2 and C_3 carbons of both of the substituted altropyranose units of the former. The simplest explanation of these observations is that the dominant 33βCD$_2$suc.PB$^+$ and 66βCD$_2$suc.PB$^+$ complexes, and their PY$^+$ analogues, have either guest complexed in a single βCD annulus in a similar way to that in βCD.PB$^+$ and βCD.PY$^+$.

A similar relationship holds for the K_1 characterizing the analogous BNS$^-$ and TNS$^-$ systems (Fig. 1),[17,18] where the more hydrophobic *t*-butyl group of BNS$^-$ interacts more strongly than does the methyl group of TNS$^-$. The magnitudes of K_1 for the PB$^+$ and PY$^+$ systems are one to four orders of magnitude less than K_1 for the BNS$^-$ and TNS$^-$ systems. This reflects the structural differences between the two types of guest, and may indicate that while the positive charge of PB$^+$ and PY$^+$ is delocalized over two dialkylamino groups, the negative charge of BNS$^-$ and TNS$^-$ is largely localized on the sulfonate group. It is noticeable that BNS$^-$ and TNS$^-$ complex substantially more strongly than PB$^+$ and PY$^+$, and that the K_1 of 66βCD$_2$suc.BNS$^-$ and 66βCD$_2$suc.TNS$^-$ are consistent with substantial cooperativity in complexation between the two linked βCD annuli.

^{1}H NMR Studies of the Dimerization and Complexation of PB$^+$ and PY$^+$

At the higher concentrations required for ^{1}H NMR studies dimerization of PB$^+$ (Eqn 2) and an analogous dimerization of PY$^+$ become significant. The H_1–H_6 resonances of PB$^+$ systematically shift upfield as $[PB^+]_{total}$ increases (Fig. 4), consistent with the formation of the $(PB^+)_2$ dimer characterized by a dimerization constant, $K_d = 100 \pm 10\,\text{mol dm}^{-3}$. Similar upfield shifts occur for the H_1–H_5 resonances of PY$^+$ consistent with the formation of $(PY^+)_2$, with a corresponding $K_d = 260 \pm 10\,\text{mol dm}^{-3}$. These upfield shifts are greatest for the PB$^+$ and PY$^+$ aromatic H_1–H_4 resonances, with the ethyl and methyl proton resonance shifts being significantly less. Accordingly, both K_d are derived from the larger δ variations of H_1–H_4, which are more accurately determined. This is consistent with H_1–H_4 experiencing an increased electron density in $(PB^+)_2$ and $(PY^+)_2$, reflecting their position in relation to the aromatic π electron density of the adjacent PB$^+$ or PY$^+$, as approximately shown in Fig. 5. The ethyl and methyl groups experience a lesser change in electron density as they are further from the aromatic π electron density. (For PB$^+$ H_1–H_6 $\delta = 8.334$, 7.680, 7.108, 6.822, 3.657, and 1.310 ppm, respectively, with the upfield shift of $(PB^+)_2$ being 1.247, 1.030, 0.849, 1.161, 0.397, and 0.251 ppm, respectively, as derived from the fitting of a dimerization algorithm to the observed δ data. For PY$^+$ H_1–H_5 $\delta = 8.305$, 7.630, 7.039, 6.654, and 3.238 ppm, respectively, with the upfield shift of $(PY^+)_2$ being 0.973, 0.082, 0.713, 1.057, and 0.033 ppm.)

For $(PY^+)_2$, K_d is 2.6 times that of $(PB^+)_2$, which suggests that of the factors likely to cause differences in dimerization: hydrophobic attraction, charge repulsion, hydration changes, and steric hindrance, the last is the most obvious, with the bulkier ethyl groups of PB$^+$ causing greater steric hindrance than the methyl groups of PY$^+$ (at the much lower concentrations used in the UV-vis and fluorescence studies dimer formation is negligible).

The complexations of PB$^+$ and PY$^+$ ($2.00 \times 10^{-3}\,\text{mol dm}^{-3}$) by βCD, 33βCD$_2$suc, and 66βCD$_2$suc over the concentration range 0–$5.00 \times 10^{-3}\,\text{mol dm}^{-3}$ were also studied under the same conditions as the dimerizations. A downfield chemical shift occurred for all PB$^+$ and PY$^+$ proton resonances, consistent with the change from the aqueous environment of their uncomplexed states to the more hydrophobic environment of their complexed states. For the 66βCD$_2$suc/PB$^+$ system, the best fit to these data was obtained for an algorithm representing equilibria (1) and (2) as shown in Fig. 6. Analogous algorithms provide the best fits to the data from the other five systems.

The downfield shifts of H_1 and H_6 of PB$^+$ in βCD.PB$^+$, 33βCD$_2$suc.PB$^+$, and 66βCD$_2$suc.PB$^+$ from H_1 and H_6 of free PB$^+$ are 0.174 and 0.094, 0.165 and 0.087, and 0.190 and 0.082 ppm, respectively; determined simultaneously with the derivation of K_1 from the observed δ data. The downfield shifts of H_1 and H_5 of PY$^+$ in βCD.PY$^+$, 33βCD$_2$suc.PY$^+$, and 66βCD$_2$suc.PY$^+$, from the corresponding values for H_1 and H_5 of free PY$^+$, are 0.078 and 0.016, 0.212 and 0.097, and 0.165 and 0.032 ppm, respectively. Because the H_1 and H_6 of PB$^+$, and the H_1 and H_5 of PY$^+$, are the most distant from each other in the two pyronines, they are likely to exhibit the largest difference in change in δ due to differences in interaction upon complexation by βCD, 33βCD$_2$suc, and 66βCD$_2$suc. In the first three cases, the downfield shift of H_1 is about twice that of H_6. In the second three cases, the downfield shift of H_1 varies from two to five times that of H_5. This is consistent with an equilibrium existing between βCD.PB$^+$ isomers (a) and (c), in which one pair of PB$^+$ ethyl groups reside in the βCD annulus and isomer, and (b), in which the PB$^+$ xanthene entity is centred in the βCD annulus (Fig. 7), such that both H_1 and H_6 experience the electronic

Table 1. Equilibrium constants for the 1:1 host/guest complexes (K_1), determined by UV-vis, fluorescence, and ^{1}H NMR spectroscopy[A]

Complex	UV-vis[B] K_1 [dm^3 mol^{-1}]	Fluorescence[B] K_1 [dm^3 mol^{-1}]	^{1}H NMR[C] K_1 [dm^3 mol^{-1}]
βCD.PB$^+$	1660 ± 80	2000 ± 100	1500 ± 150
33βCD$_2$suc.PB$^+$	4200 ± 200	4600 ± 200	4400 ± 200
66βCD$_2$suc.PB$^+$	4500 ± 200	4900 ± 200	5400 ± 200
βCD.PY$^+$	370 ± 20	320 ± 30	320 ± 70
33βCD$_2$suc.PY$^+$	760 ± 40	830 ± 40	500 ± 50
66βCD$_2$suc.PY$^+$	780 ± 40	740 ± 40	500 ± 50
βCD.BNS$^-$	55400[D]	46500[D]	
33βCD$_2$suc.BNS$^-$	186000[D]	110000[D]	
66βCD$_2$suc.BNS$^-$	1250000[D]	3300000[D]	
βCD.TNS$^-$	3020[E]	3300[E]	
33βCD$_2$suc.TNS$^-$	10700[E]	9600[E]	
66βCD$_2$suc.TNS$^-$	16100[E]	12500[E]	

[A]For PB$^+$, PY$^+$, and BNS$^-$, $K_d = 100 \pm 10$, 260 ± 10, and 265 dm^3 mol^{-1}, respectively.
[B]In aqueous 1.00×10^{-4} mol dm^{-3} hydrochloric acid at $I = 0.10$ mol dm^{-3} (NaCl) and 298.2 K.
[C]In 1.00×10^{-4} mol dm^{-3} hydrochloric acid D_2O solution at $I = 0.10$ mol dm^{-3} (NaCl) and 298.2 K.
[D]In aqueous phosphate buffer at pH 7.0 and $I = 0.1$ mol dm^{-3} and 298.2 K from ref. [17].
[E]In aqueous phosphate buffer at pH 7.0 and $I = 0.1$ mol dm^{-3} and 298.2 K from ref. [18].

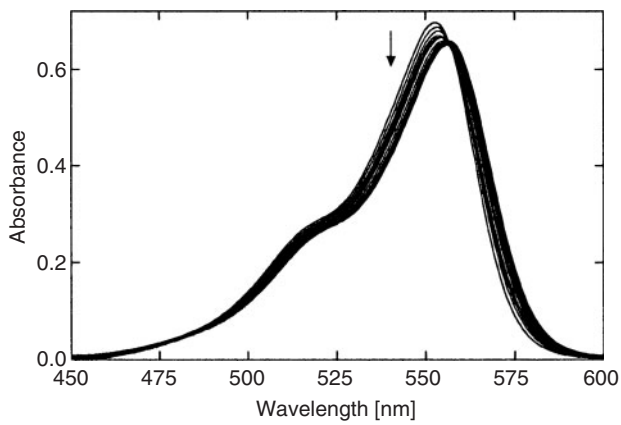

Fig. 2. UV-vis absorbance spectra of PB$^+$ alone (6.51×10^{-6} mol dm^{-3}) and in the presence of increasing concentrations of 33βCD$_2$suc (ranging from 0.00 to 1.97×10^{-3} mol dm^{-3}) in aqueous hydrochloric acid (1.00×10^{-4} mol dm^{-3}, $I = 0.10$ mol dm^{-3} NaCl) at 298.2 K. The arrow indicates the direction of absorbance change as [33βCD$_2$suc]$_{total}$ increases. An isosbestic point occurs at 556 nm. $\lambda_{max} = 553$ nm ($\varepsilon = 1.07 \times 10^5$ dm^3 mol^{-1} cm^{-1}) and 557 nm ($\varepsilon = 1.01 \times 10^5$ dm^3 mol^{-1} cm^{-1}) for the free and complexed PB$^+$ species, respectively.

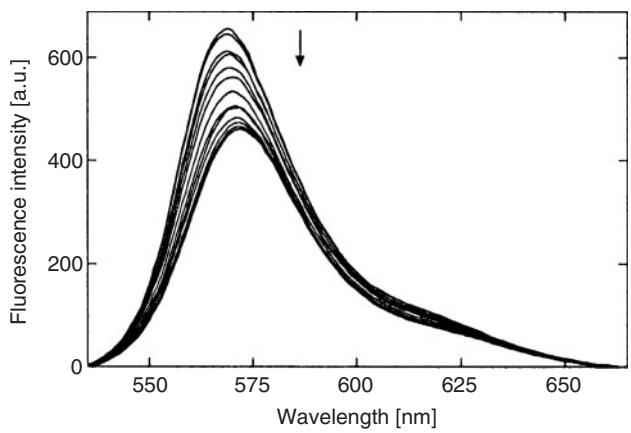

Fig. 3. Emission spectra of PB$^+$ alone (6.19×10^{-7} mol dm^{-3}) and in the presence of increasing concentrations of 33βCD$_2$suc (ranging from 0.00 to 1.54×10^{-3} mol dm^{-3}) in aqueous hydrochloric acid (1.00×10^{-4} mol dm^{-3}, $I = 0.10$ mol dm^{-3} NaCl) at 298.2 K. The excitation wavelength $\lambda_{ex} = 515$ nm. The excitation and emission slit widths = 5 nm. The arrow indicates the direction of relative fluorescence emission change as [33βCD$_2$suc]$_{total}$ increases. The $\lambda_{max} = 568$ nm (656 a.u.) and 572 nm (431 a.u.) for the free and complexed PB$^+$ species, respectively.

environment of the βCD annulus (the resulting inequivalence of the two *N*-diethyl groups is not observed in the ^{1}H spectra as the complex lifetimes are short on the ^{1}H NMR timescale). Alternatively, a dominant βCD.PB$^+$ complex with a structure midway between either (a) and (b), or (b) and (c), or both may exist. Similar possibilities exist for the complexation of PB$^+$ in single βCD annuli of 33βCD$_2$suc.PB$^+$ and 66βCD$_2$suc.PB$^+$ and for the analogous PY$^+$ systems.

2D ROESY ^{1}H NMR Studies

Solutions of PB$^+$ (2.00×10^{-3} mol dm^{-3}) in the presence of either double the concentration of native βCD, or equimolar in either of the linked βCD dimers in D_2O solution, show ^{1}H ROESY NMR cross-peaks arising from interactions between the βCD H_3, H_5, and H_6 annular protons and the H_6 and H_4 protons of PB$^+$ (those arising from the PB$^+$ H_5 protons are obscured due their chemical shift being similar to those of βCD protons) as seen in Fig. 8. This is consistent with the two sets of interacting protons being within 400 p.m. of each other and the ethyl groups of PB$^+$ and the attached aromatic ring being partially within the βCD annulus of the dominant βCD.PB$^+$ host-guest complex. Because the ratio of methyl protons to aromatic protons is 6:1, the cross-peaks arising from the methyl protons will be the more intense if all other factors are the same. Similar spectra are observed for the 33βCD$_2$suc.PB$^+$ (Fig. 9) and 66βCD$_2$suc.PB$^+$ host-guest complexes. Similar cross-peaks are also observed for the analogous PY$^+$ solutions, but are weaker, consistent with the PY$^+$ complexes exhibiting lower K_1 values. These data correlate well with either of the models proposed, on the basis of the

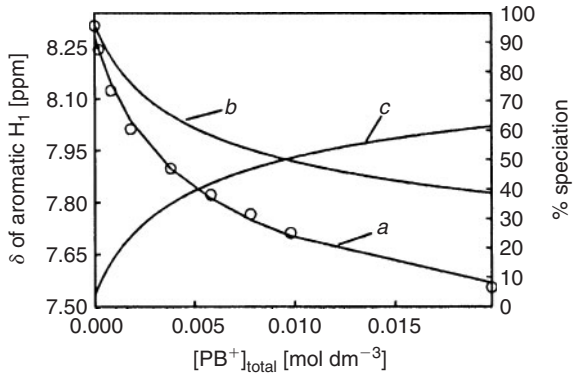

Fig. 4. The left ordinate shows the variation of δ ^{1}H (300 MHz) of the aromatic H_1 proton of PB^+ as $[PB^+]_{total}$ increases from 2.00×10^{-4} mol dm^{-3} to 2.00×10^{-2} mol dm^{-3} in D_2O (1.00×10^{-4} mol dm^{-3} hydrochloric acid, $I = 0.10$ mol dm^{-3} NaCl) at 298.2 K. The circles represent experimental data. The solid curve *a*, shows the simultaneous best fit of the algorithm for dimerization of PB^+ to the δ variations of protons H_1–H_4. The right-hand ordinate shows the percentage speciation relative to $[PB^+]_{total}$. Curve *b* shows the percentage of $[PB^+]$ and curve *c* represents twice the percentage of $[(PB^+)_2]$.

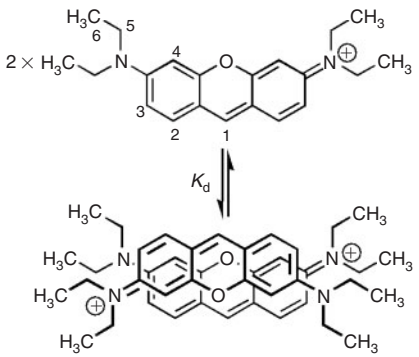

Fig. 5. Dimerization of PB^+ to form $(PB^+)_2$.

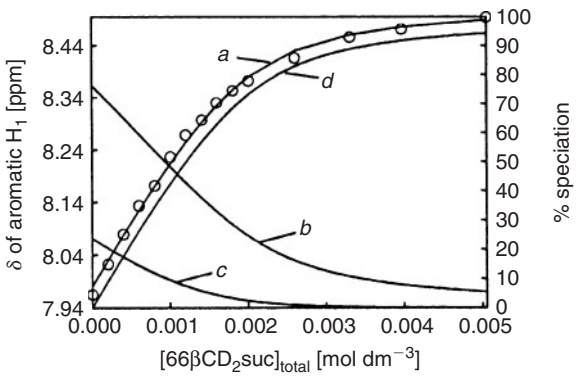

Fig. 6. Left ordinate: variation of δ ^{1}H (300 MHz) of the aromatic H_1 of PB^+ (2.00×10^{-3} mol dm^{-3}) with $[66\beta CD_2suc]_{total}$ (ranging from 0 to 5.00×10^{-3} mol dm^{-3}) in D_2O (1.00×10^{-4} mol dm^{-3} hydrochloric acid, $I = 0.10$ mol dm^{-3} NaCl) at 298.2 K. The circles are the experimental data and the solid curve *a* is the best fit of the algorithm incorporating $(PB^+)_2$ and $66\beta CD_2suc.PB^+$ to the δ variations of protons H_1–H_4 and H_6. Right ordinate: speciation relative to $[PB^+]_{total}$, curve *b* is the percentage of $[PB^+]$, curve *c* is twice the percentage of $[(PB^+)_2]$, and curve *d* is the percentage of $[66\beta CD_2suc.PB^+]$.

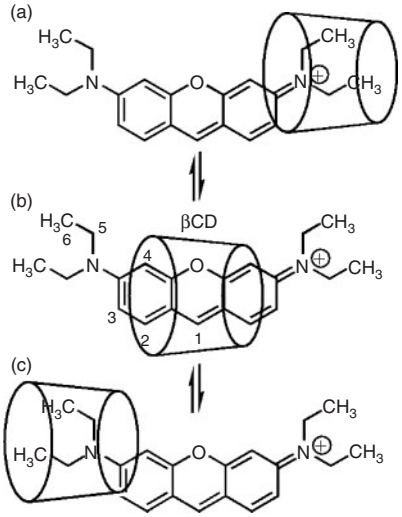

Fig. 7. Possible equilibria between $\beta CD.PB^+$ isomers (a)–(c).

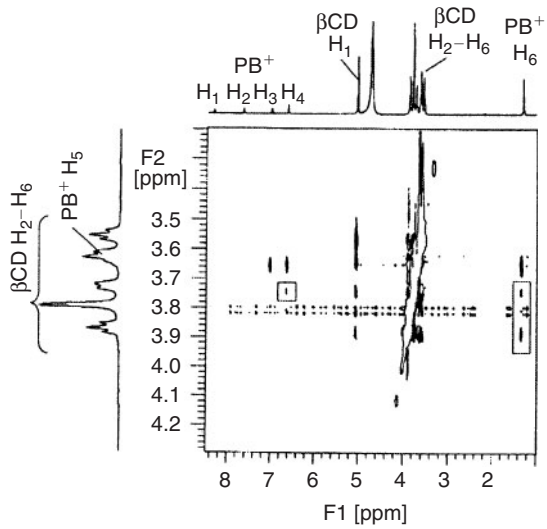

Fig. 8. 2D ^{1}H ROESY NMR (600 MHz) spectrum of PB^+ (2.00×10^{-3} mol dm^{-3}) with two molar equivalent βCD in D_2O (1.00×10^{-4} mol dm^{-3} hydrochloric acid, $I = 0.10$ mol dm^{-3} NaCl) at 298.2 K, with a mixing time of 300 ms. Cross-peaks between H_6 of PB^+ and H_3, H_5, and H_6 of βCD; and between H_4 of PB^+ and H_5 of βCD, are enclosed in rectangles. The other cross-peaks arise from interactions between the H_1 and H_2–H_6 of βCD and between H_3, H_4 and H_6 and H_5 of PB^+.

PB^+ and PY^+ chemical shift variations discussed in the previous section.

The deductions from the ^{1}H NMR data concerning the complexation of PB^+ and PY^+ are relevant to interpretation of the resulting fluorescence quenching. Both the model for complexation (Fig. 7) and the alternative model, where a dominant $\beta CD.PB^+$ complex with a structure midway between either (a) and (b), or (b) and (c), or both may exist, are likely to alter the symmetry of the charge distribution represented by the PB^+ and PY^+ resonance structures (d)–(g) (Fig. 10), through which all bonds share partial double bond character. Complexation by βCD, $33(\beta CD)_2suc$, and $66(\beta CD)_2suc$ results in part of PB^+ and PY^+ being in the hydrophobic βCD annulus and part in the aqueous environment. As both dialkylamino groups cannot be

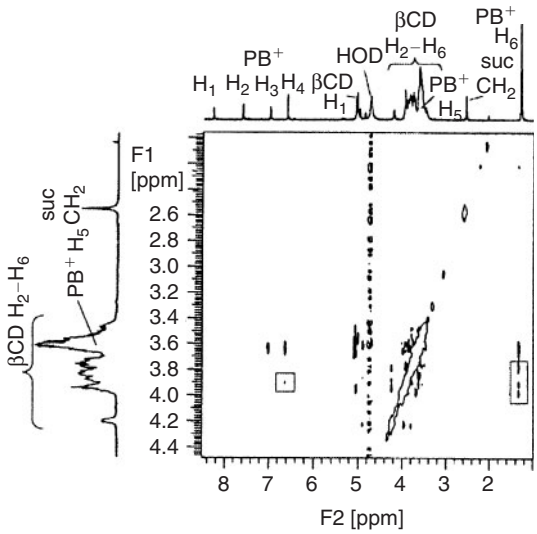

Fig. 9. 2D ^{1}H ROESY NMR (600 MHz) spectrum of PB^+ (2.00×10^{-3} mol dm^{-3}) and equimolar 33(βCD)$_2$suc in D_2O (1.00×10^{-4} mol dm^{-3} hydrochloric acid, $I = 0.10$ mol dm^{-3} NaCl) at 298.2 K, with a mixing time of 300 ms. The cross-peaks enclosed in rectangles arise from interactions between H_6 of PB^+ and H_3, H_5, H_6 of βCD; and between H_4 of PB^+ and H_5 of βCD. The other cross-peaks arise from interactions between the H_1 and H_2–H_6 of 33(βCD)$_2$suc and between H_3, H_4 and H_6 and H_5 of PB^+.

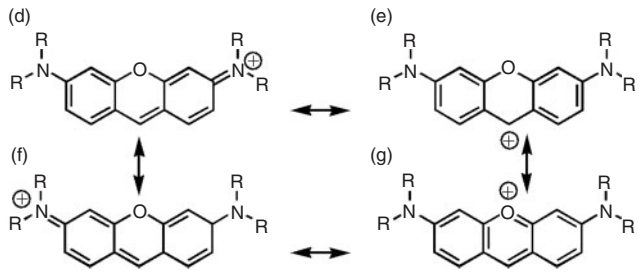

Fig. 10. Resonance structures (d)–(g) of PB^+, R = CH_2CH_3, and PY^+, R = CH_3.

simultaneously in the βCD annulus, both PB^+ and PY^+ experience an environmental asymmetry which is likely to introduce an asymmetry in charge distribution. As complexation causes fluorescence quenching the resulting change in charge distribution must increase the probability of non-radiative decay of the excited states of PB^+ and PY^+.

Two studies in a range of solvents are consistent with the most probable non-radiative decay for PB^+ and PY^+ occurring through a two-state mechanism, where the fluorescent planar states, resembling (d) and (f), are in equilibrium with non-emissive states, resembling (e) and (g), in which nitrogen assumes a tetrahedral stereochemistry such that an S_1–S_0 internal conversion occurs.[14,15] A similar pathway for non-radiative transitions of excited electronic states of PB^+ and PY^+ to their ground states provides a plausible explanation for the decrease in fluorescence shown by PB^+ and PY^+ upon complexation by βCD, 33(βCD)$_2$suc, and 66(βCD)$_2$suc.

A model has also been proposed by Reija for the decreased fluorescence of PB^+ and PY^+ upon complexation by βCD.[16] It is postulated that the xanthene entities of PB^+ and PY^+ are completely complexed inside the βCD annulus to form a non-emissive, charge-transfer excited state where the positive charge is located at the centre of the xanthene entity as a consequence of stabilization by the electron rich environment generated by the ether oxygens of the βCD annulus. This accentuates a structural change in the amino groups towards a tetrahedral stereochemistry, which engenders non-radiative deactivation. This model was proposed in the absence of evidence for the substantial interaction of the dialkylamino groups of PB^+ and PY^+ with the interior of the βCD annulus shown to occur in the present study. In view of this it is apparent that Reija's model represents a component of the two alternative models proposed here for introducing asymmetry into the charge distribution in PB^+ and PY^+ upon complexation by βCD, 33βCD$_2$suc, and 66βCD$_2$suc, and consequent fluorescence quenching.

Conclusions

The complexation of PB^+ and PY^+ by βCD, 33βCD$_2$suc, and 66βCD$_2$suc have been characterized in aqueous solution by UV-vis, fluorescence, and ^{1}H NMR spectroscopy. By comparison with the stabilities of the βCD.PB^+ and βCD.PY^+, 66βCD$_2$suc.PB^+, 33βCD$_2$suc.PB^+, and the analogous PY^+ complexes, are slightly more than twice as stable, consistent with a statistical enhancement in stability and little cooperativity between the two linked βCD annuli in complexing PB^+ and PY^+. However, PB^+ is complexed approximately five times more strongly than PY^+, consistent with the greater hydrophobicity of the PB^+ ethyl groups interacting more strongly with the hydrophobic annuli of βCD, 33βCD$_2$suc, and 66βCD$_2$suc, than do the methyl groups of PY^+. The fluorescence quenching of PB^+ and PY^+ in the complexes is attributed to a change in their charge distribution, such that non-emissive relaxation of the excited state occurs through an dialkylamino group, assuming a tetrahedral stereochemistry in the complexes than is the case in free PB^+ and PY^+. The dimerizations of PB^+ and PY^+, which occurs at the higher concentrations required for ^{1}H NMR studies, have also been characterized.

Experimental

Materials

Pyronine B (Sigma) was purchased as the 95% pure salt $(PB)_2Fe_2Cl_8$ and was twice recrystallized from water before use.[19] The commercially obtained pyronine Y chloride salt contained ~40% impurities by weight. These water insoluble impurities were filtered from an aqueous slurry with a 0.45 μm filter before use.[12] β-Cyclodextrin (Nihon Shokuhin Kako Co) was used without further purification and 33βCD$_2$suc and 66βCD$_2$suc were synthesized as previously described.[20] Hydrochloric acid (Ajax) and sodium chloride (Merck) were used to maintain constant acidity and ionic strength. Water was purified with a Milli-Q system. All organic solvents were of HPLC grade.

Solutions were prepared from fresh stock solutions and were 1.00×10^{-4} mol dm^{-3} in hydrochloric acid, to prevent the base hydrolysis of PB^+ and PY^+,[16] and 0.10 mol dm^{-3} NaCl to maintain a constant ionic strength. The concentrations of PY^+ stock solutions were estimated using the reported molar absorptivity at 546 nm of $\varepsilon = 8.1 \times 10^4$ mol^{-1} dm^3 cm^{-1}.[21] Aqueous solutions for UV-visible and fluorescence studies were 6.0×10^{-6} mol dm^{-3} in PB^+ and 9.0×10^{-6} mol dm^{-3} in PY^+; and 6.0×10^{-7} mol dm^{-3} of PB^+ and 9.0×10^{-7} mol dm^{-3} of PY^+, respectively. The βCD and linked βCD dimer concentrations varied over wide ranges, as indicated in the figure captions. Solutions for ^{1}H NMR experiments were prepared in D_2O

1.00×10^{-4} mol dm^{-3} in hydrochloric acid and 0.10 mol dm^{-3} in NaCl. The concentrations of PB^+ and PY^+ solutions for dimerization studies ranged from 1.0×10^{-3} mol dm^{-3} to 2.0×10^{-2} mol dm^{-3}. For complexation studies the concentrations of PB^+ and PY^+ were 2.0×10^{-3} mol dm^{-3}, while those of the βCD and dimer hosts were varied over the range 0–5.0×10^{-3} mol dm^{-3}. For the 2D ^{1}H NMR ROESY experiments, each sample was 2.0×10^{-3} mol dm^{-3} in either PB^+ or PY^+ and in either βCD or a linked βCD dimer.

Instrumental

UV-vis spectra were run on a Varian Cary 5000 spectrophotometer, using matched quartz cells with a 1 cm path length, in a cell block with a constant temperature of 298.2 K. Solutions were equilibrated at this temperature before scanning. The scan rate was 600 nm min^{-1} and the data interval was 0.5 nm. Fluorescence spectra were run on a Varian Cary Eclipse fluorimeter. The solutions were equilibrated in a 1 cm path length quartz cell in a thermostatted 298.2 K cell block. The excitation and emission slit widths were 5 nm, the scan rate was 120 nm min^{-1}, and the data interval was 0.5 nm. 2D ^{1}H ROESY NMR spectra were recorded on a Varian Inova 600 spectrometer operating at 599.957 MHz, using a standard pulse sequence with a mixing time of 300 ms.

Data Analysis

The K_1 for the 1:1 host-guest complexes of either PB^+ or PY^+ with the βCD and linked βCD dimer hosts were derived by simultaneously fitting the absorbance variation typified by Fig. 1 over a wide wavelength range at 0.5 nm intervals to Eqn 3:

$$A = \varepsilon_{PB}[PB^+] + \varepsilon_{33\beta CD2suc}[33\beta CD_2suc] + \varepsilon_{33\beta CD2suc.PB}[33\beta CD_2suc.PB^+], \quad (3)$$

where A is the absorbance and ε_{PB}, $\varepsilon_{33\beta CD2suc}$, $\varepsilon_{33\beta CD2suc.PB}$ are the molar absorbances of the PB^+, $33\beta CD_2suc$, and $33\beta CD_2suc.PB^+$, respectively. Analogous equations apply for the absorbance variation of the other five systems and for the fluorescence variations all six systems. The *SPECFIT/32* protocol was used in the fitting procedure.[22] The dimerization constants, K_d, for PB^+ and PY^+ were derived by simultaneously fitting the variation of the ^{1}H chemical shifts, δ_{exp}, of H_1–H_4 as $[PB^+]_{total}$ and $[PY^+]_{total}$ increased to Eqn 4, where the third right hand term is absent, to the experimental data using the *HypNMR 2003* program as typified by Fig. 4.[23,24] The K_1 for all six systems were similarly derived by fitting ^{1}H chemical shift variations for H_1–H_4 to Eqn 4 for the $66\beta CD_2suc.PB^+$ system (Fig. 6) and analogous equations for the other five systems.

$$\delta_{exp} = \delta_{PB}[PB^+] + \delta_{PB2}[(PB^+)_2] + \delta_{\beta CD2suc.PB}[66\beta CD_2suc.PB^+] \quad (4)$$

Accessory Publication

Electronic supplementary material is available showing: (i) UV-vis and fluorescence changes of PB^+ and PY^+ and fitting of algorithms to these data to derive complexation constants and speciation plots; (ii) ^{1}H NMR chemical shift variations of PB^+ and PY^+ and fitting of algorithms to these data to derive dimerization and complexation constants; (iii) 2D ROESY ^{1}H NMR spectra and a Table of ^{1}H NMR chemical shifts. This material is available on the Journal's website.

Acknowledgement

Support of this study by the Australian Research Council and the University of Adelaide, and the award of an Endeavour Postgraduate Award to H.T.N. are gratefully acknowledged.

References

[1] J. Szejtli, *Chem. Rev.* **1998**, *98*, 1743. doi:10.1021/CR970022C
[2] C. J. Easton, S. F. Lincoln, *Modified Cyclodextrins: Scaffolds and Templates for Supramolecular Chemistry* **1999** (Imperial College Press: London).
[3] A. Harada, *Acc. Chem. Res.* **2001**, *34*, 456. doi:10.1021/AR000174L
[4] Y. Liu, Y. Chen, *Acc. Chem. Res.* **2006**, *39*, 681. doi:10.1021/AR0502275
[5] J. Szejtli, *Chem. Rev.* **1998**, *98*, 1743. doi:10.1021/CR970022C
[6] A. R. Hedges, *Chem. Rev.* **1998**, *98*, 2035. doi:10.1021/CR970014W
[7] E. M. M. Del Valle, *Process Biochem.* **2004**, *39*, 1033. doi:10.1016/S0032-9592(03)00258-9
[8] T. Loftsson, D. Duchêne, *Int. J. Pharmaceutics* **2007**, *329*, 1. doi:10.1016/J.IJPHARM.2006.10.044
[9] J. H. Coates, C. J. Easton, S. J. van Eyk, S. F. Lincoln, B. L. May, C. B. Whalland, M. L. Williams, *J. Chem. Soc., Perkin Trans. 1* **1990**, 2619. doi:10.1039/P19900002619
[10] K. Fujiki, C. Iwanaga, M. Koizumi, *Bull. Chem. Soc. Jpn.* **1962**, *35*, 185. doi:10.1246/BCSJ.35.185
[11] R. L. Schiller, S. F. Lincoln, J. H. Coates, *J. Chem. Soc., Faraday Trans. I* **1986**, *82*, 2123 (in the text "annular radii" should read "annular diameters"). doi:10.1039/F19868202123
[12] R. L. Schiller, S. F. Lincoln, J. H. Coates, *J. Chem. Soc., Faraday Trans. I* **1987**, *83*, 3237. doi:10.1039/F19878303237
[13] R. L. Schiller, S. F. Lincoln, J. H. Coates, *J. Incl. Phenom.* **1987**, *5*, 59. doi:10.1007/BF00656403
[14] Y. Onganer, E. L. Quitevis, *J. Phys. Chem.* **1992**, *96*, 7996. doi:10.1021/J100199A033
[15] B. Acemioglu, M. Arik, Y. Onganer, *J. Lumin.* **2002**, *97*, 153. doi:10.1016/S0022-2313(02)00218-1
[16] B. Reija, W. Al-Soufi, M. Novo, J. V. Tato, *J. Phys. Chem. B* **2005**, *109*, 1364. doi:10.1021/JP046587B
[17] D.-T. Pham, P. Clements, C. J. Easton, J. Papageorgiou, B. L. May, S. F. Lincoln, *New J. Chem.* **2008**, *32*, 712. doi:10.1039/B715985D
[18] D.-T. Pham, P. Clements, C. J. Easton, J. Papageorgiou, B. L. May, S. F. Lincoln, *Supramol. Chem.* **2009**, *21*, 510. doi:10.1080/10610270802406579
[19] E. M. Chamberlin, B. F. Powell, D. E. Williams, J. Conn, *J. Org. Chem.* **1962**, *27*, 2263. doi:10.1021/JO01053A538
[20] C. J. Easton, S. J. van Eyk, S. F. Lincoln, B. L. May, J. Papageorgiou, M. J. Williams, *Aust. J. Chem.* **1997**, *50*, 9. doi:10.1071/C96168
[21] L. P. Glanneschi, T. Kurucsev, *J. Chem. Soc., Faraday Trans. II* **1974**, *70*, 1334. doi:10.1039/F29747001334
[22] R. A. Binstead, B. Jung, A. D. Zuberbuhler, *SPECFIT/32*, *v3.0.39(b)* **2007** (Spectrum Software Associates: Marlborough, MA, USA).
[23] C. Frassineti, S. Ghelli, P. Gans, A. Sabatini, S. Moruzzi, A. Vacca, *Anal. Biochem.* **1995**, *231*, 374. doi:10.1006/ABIO.1995.9984
[24] P. Gans, A. Sabatini, A. Vacca, *HypNMR*, *v3.1.5* **2004** (Protonic Software).